Epstein-Barr virus-associated lymphoepithelial carcinoma arising in the parotid gland: A case report and literature review

AKINOBU KUBOTA[1,2], NOBUYUKI BANDOH[1], TAKASHI GOTO[1], KEN-ICHI MATSUMOTO[3], TOMOMI YAMAGUCHI-ISHOCHI[4], YASUTAKA KATO[4], HIROSHI NISHIHARA[5] and HIDEHIRO TAKEI[6]

[1]Department of Otolaryngology-Head and Neck Surgery, Hokuto Hospital, Obihiro, Hokkaido 080-0833; [2]Department of Otolaryngology-Head and Neck Surgery, Asahikawa Medical University, Asahikawa, Hokkaido 078-8510; Departments of [3]Radiation Therapy and [4]Pathology and Genetics, Hokuto Hospital, Obihiro, Hokkaido 080-0833; [5]Keio Cancer Center, Keio University School of Medicine, Tokyo 160-8582, Japan; [6]Department of Pathology and Translational Pathobiology, Louisiana State University Health Sciences Center at Shreveport, Shreveport, LA 71103, USA

Received December 29, 2022; Accepted January 30, 2023

DOI: 10.3892/mco.2023.2620

Abstract. A 60-year-old woman presented with a 3-year history of a slow-growing, painless mass in their left parotid gland. Ultrasonography revealed a well-circumscribed, lobulated, hypoechoic mass measuring 19x12x10 mm in the left parotid gland. Computed tomography revealed a well-circumscribed, solid mass with homogeneous enhancement. Fluorodeoxyglucose-positron emission tomography revealed uptake by the tumor but no uptake in other organs, including the nasopharynx. The patient underwent superficial parotidectomy with adequate safety margins and selective neck dissection followed by radiotherapy. No facial paralysis or recurrence of the tumor had been observed as of 20 months post-operation. Histologically, the tumor was composed of sheets of syncytial cancer cells with prominent nucleoli in a dense lymphoplasmacytic background. Epstein-Barr virus (EBV)-encoded RNA *in situ* hybridization was diffusely positive in the tumor cells. These findings indicated that the tumor was an EBV-associated lymphoepithelial carcinoma. Metastasis, especially from the nasopharynx, was excluded endoscopically and radiologically. Targeted next-generation sequencing of 160 cancer-related genes using the surgical specimen revealed no mutations, including known significant mutations detected in EBV-associated nasopharyngeal carcinoma.

Correspondence to: Dr Nobuyuki Bandoh, Department of Otolaryngology-Head and Neck Surgery, Hokuto Hospital, 7-5 Inadacho Kisen, Obihiro, Hokkaido 080-0833, Japan
E-mail: bando@hokuto7.or.jp

Key words: lymphoepithelial carcinoma, parotid gland, Epstein-Barr virus, next generation sequencing

Introduction

Lymphoepithelial carcinoma (LEC), according to the current World Health Organization Classification, is one of 21 subtypes of salivary malignant epithelial tumors and is histologically an undifferentiated carcinoma with a syncytial growth pattern accompanied by prominent non-neoplastic lymphoplasmacytic infiltrates, mostly associated with Epstein-Barr virus (EBV) infection (1,2). These histological features are indistinguishable from those of undifferentiated nasopharyngeal carcinoma (NPC), which is also associated with EBV infection. LEC arising in the salivary glands is extremely rare, comprising only 0.4% of salivary carcinomas (3). Thus, the information on this tumor is limited to case reports and small case series, most of which described patients from Arctic Inuit (Eskimo), Southern Chinese, and Japanese populations with strong EBV involvement (1). Given its rarity, neither the etiology nor clinical features of LEC of the salivary gland have been fully elucidated. Here, we report a rare case of EBV-associated LEC arising in the parotid gland, which was treated with surgery followed by radiotherapy. Somatic mutation test using next generation sequencing (NGS) was also performed and showed no evidence of any mutations.

Case report

A 60-year-old Japanese woman with a 3-years history of a slow-growing, painless mass in her left parotid gland was admitted to our department. She had no medical or familial history of note. A thumb-sized, hard mass was palpated on the left parotid gland (Fig. 1A). No facial palsy was observed. Endoscopic examination did not reveal any tumorous lesions in the nasopharynx. Ultrasonography revealed a well-circumscribed, lobulated, hypoechoic mass with posterior enhancement measuring 19x12x10 mm in the left parotid gland (Fig. 1B). Computed tomography (CT) revealed a well-circumscribed, solid mass exhibiting homogeneous enhancement in the posterior part of the left parotid gland (Fig. 1C). No abnormal enlargement of lymph nodes was

identified. Fluorodeoxyglucose-positron emission tomography (FDG-PET)/CT revealed uptake by the tumor, but not in other areas including the nasopharynx (Fig. 1D). Fine-needle aspiration cytology (FNAC) demonstrated numerous irregularly shaped trabecular clusters of relatively large cancer cells with vesicular chromatin and prominent 'cherry-red' nucleoli (Fig. 2A). Lymphocytic infiltrate was not conspicuous. Cytologically, poorly differentiated carcinoma was suggested. The patient underwent left superficial parotidectomy with adequate safety margins. After making an S-shaped incision, the facial nerve was identified and preserved. The adjacent portion of the sternocleidomastoid muscle was resected, and selective neck dissection of Level II was added. Her clinical course proved uneventful. Postoperatively, the patient received radiotherapy to the parotid gland area at 50 Gy and then has been screened with ultrasonography and CT scan at fixed intervals. No evidence of recurrence has been observed as of 20 months postoperatively.

Histologically, a well-circumscribed, encapsuled nodule was composed of sheets and cords of relatively large cancer cells with vesicular nuclei, prominent nucleoli, and indistinct cell borders (Fig. 2B). Scattered mitotic figures were observed. The sheets and cords of tumor were intermingled with abundant lymphoplasmacytic infiltrate with secondary lymphoid follicles (Fig. 2C). No neck lymph node metastasis was identified. Surgical margins were negative for malignancy. Immunoperoxidase staining of formalin-fixed, paraffin-embedded (FFPE) tissue sections with anti-keratin/cytokeratin monoclonal antibody (clone AE1/AE3; Nichirei Biosciences) was performed using a Ventana OptiView DAB IHC detection kit (Roche Diagnostics). Tumor cells were positive for AE1/AE3 (Fig. 2D) and negative for human epidermal growth factor receptor-2, androgen receptor, S-100 protein, α-smooth muscle actin, synaptophysin, and chromogranin (data not shown). *In situ* hybridization for EBV-encoded RNA (EBER) on FFPE tissue sections was assessed by using a fluorescein isothiocyanate-conjugated EBER peptide nucleic acid (PNA)-probe (DaKoCytomation, Glostrup, Denmark) and PNA *in situ* hybridization detection kit (DaKoCytomation) according to the manufacturer's instructions. Diffuse nuclear staining was observed in the tumor cells (Fig. 2E). These histologic features, immunohistochemical profile, and *in situ* hybridization for EBER were those of an EBV-associated LEC, pT1N0M0, pStage I on the 8th edition of the AJCC/TNM staging system (4).

Blood examination showed high levels of serum anti-viral capsid antigen (VCA) immunoglobulin (Ig)G (1:10.6) and anti-EBV-nuclear antigen (EBNA) IgG (1:4) antibodies, and negative results for anti-VCA IgA, anti-VCA IgM, and anti-early antigen (EA) IgG antibodies. Targeted-NGS was performed as previously described (5). Briefly, total DNA was extracted from FFPE tissue sections using a Maxwell 16 FFPE Plus LEV DNA purification kit (Promega). Amplicon sequencing of targeted regions of 160 cancer-related genes (Table SI) was carried out using the GeneRead DNAseq Targeted Panels V2 Human Clinically Relevant Tumor Panel (NGHS-101X; Qiagen). Libraries were sequenced using an Illumina MiSeq platform (Illumina). Raw read data obtained from the amplicon sequencing were processed using online analytical resources from the GeneRead DNAseq Variant Calling Service for analysis of mutations. No mutations, including known significant mutations reported in NPC (6), were identified.

Discussion

Clinical characteristics of 27 patients with EBV-associated LEC arising in the parotid gland that have been described in the literature with detailed information since 2005, including the present case, are shown in Table I (7-18). These tumors occurred across a wide age range (21-67 years; median, 46 years), and a female predominance was evident (17 females, 10 males). Swelling in the parotid area as clinical presentation was seen in all 27 patients. In addition, three patients (11%) showed facial nerve palsy and only one (4%) showed a painful mass. The time intervals from first symptom to treatment ranged from 3 to 72 months (median, 11 months). Maximum lesion diameters ranged from 15 to 93 mm.

Ultrasonographically, LEC lesions have been described as a hypoechoic solid mass with posterior enhancement and increased vascularity on color Doppler images (12). On CT scan, the lesions have been depicted as exophytic, solid masses with good contrast enhancement in the parotid gland (12). Fifteen of 27 patients (56%) with EBV-associated LEC revealed neck lymph node metastasis (Table I). Identification of enlarged lymph nodes by imaging studies should merit consideration of neck lymph node dissection.

FNAC diagnosis of parotid LEC is challenging given its rarity. In the previous reports, FNAC could not make the definitive diagnosis of LEC in any cases and the interpretation included carcinomas in 7 patients, lymphoma in 1 patient, and benign lesions in 3 patients (Table I). Cytologic features of LEC described are large, single and clustered, polygonal and spindle-shaped tumor cells with a high nucleus-to-cytoplasm ratio in syncytial sheets (3,19). The nuclei are vesicular with prominent nucleoli. Most display a prominent mixed lymphoid population that may mask the epithelial elements, resulting in misdiagnosis of lymphoid entities such as lymphoma. In the present case, FNAC revealed findings of a poorly differentiated carcinoma but could not suggest LEC due to its scarcity of lymphocytes. With cell block material from the tumor available, differential diagnosis could have been narrowed down based on positivity for EBER *in situ* hybridization (19). Stage of the disease was Stage I in 5 (21%), Stage II in 4 (17%), Stage III in 2 (8%), Stage IVa in 7 (30%), and Stage IVb in 6 (25%) of the 24 patients.

Histologically, LEC consists of infiltrative sheets, islands and cords of cancer cells that are separated by dense lymphoid stroma. The tumor cells are characterized by indistinct cell borders (i.e., syncytial), lightly eosinophilic cytoplasm, oval moderately pleomorphic vesicular nuclei with conspicuous nucleoli (1). Immunohistochemical examination is of great help in the diagnosis of LEC. Epithelial markers such as AE1/AE3 highlight cancer cells that might be markedly obscured by densely infiltrating lymphocytes and plasma cells. The main differential includes metastasis from either NPC or lymphoepithelial-like carcinoma arising in other organs (e.g., stomach) to not only parotid parenchyma but also to intraglandular lymph node. In the present case, endoscopic examination of the nasopharynx and FDG-PET/CT excluded metastasis.

Figure 1. Imaging findings of the tumor. (A) A thumb finger-sized, hard mass is palpated on the left parotid gland. (B) Ultrasonography reveals a lobulated, well-circumscribed, hypoechoic mass exhibiting heterogeneity in the left parotid gland, measuring 19x12x10 mm. (C) CT reveals a well-circumscribed, solid mass with homogenous enhancement in the posterior part of the superficial lobe of the left parotid gland. (D) Fluorodeoxyglucose-positron emission tomography/CT reveals uptake by the tumor. The tumor is indicated by arrowheads. CT, computed tomography.

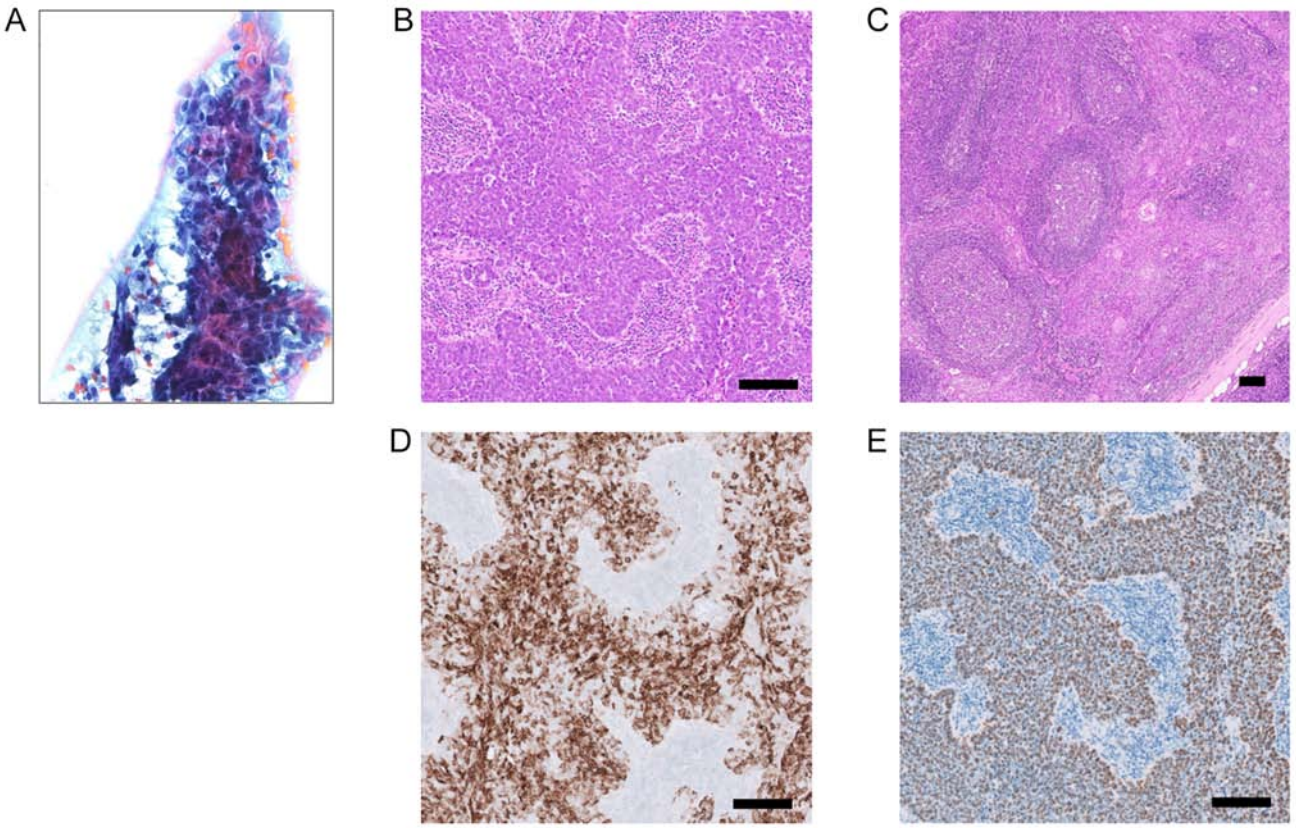

Figure 2. Histologic findings of the tumor. (A) Fine-needle aspiration cytology demonstrates overlapping, irregularly shaped clusters that are composed of relatively large, atypical cells with vesicular chromatin and prominent nucleoli. (B) A well-circumscribed, encapsuled nodule is composed of sheets and cords of relatively large cancer cells with vesicular nuclei, prominent nucleoli, and indistinct cell borders. (C) The sheets and cords of tumor are intermingled with abundant lymphoplasmacytic infiltrate with secondary lymphoid follicles. (D) Tumor cells are positive for AE1/AE3. (E) *In situ* hybridization for Epstein-Barr virus-encoded RNA shows diffuse nuclear staining in tumor cells. All scale bars, 100 μm.

Identification of EBV infection is not essential for the diagnosis of LEC in the parotid glands; however, if found to be associated with EBV infection, such parotid carcinoma is highly suggestive of LEC especially when there is no known carcinoma elsewhere in the body. Parotid LEC in the endemic areas was nearly 100% associated with EBV (3), suggesting a strong relationship between EBV infection and its tumorigenesis. Progression of LEC may involve malignant transformation of glandular or ductal inclusions in intraparotid gland lymph nodes or transformation of benign lymphoepithelial lesions (3). EBV-associated NPC is characterized by the lymphoepithelial features, suggesting that lymphoid infiltrate may represent a host immune reaction to the EBV-associated antigens expressed on the tumor cells (20). Our case also demonstrated dense lymphoplasmacytic infiltrate not only in the stroma but within the sheets/nests of tumor cells. In the present case, blood examination showed high levels of serum anti-VCA IgG and anti-EBNA IgG antibodies, and negative results for anti-VCA IgA and anti-EA IgG antibodies, suggesting a latent viral infection of EBV. This is different from the pattern of NPC, which shows positive results for serum anti-VCA-IgA and anti-EA-IgG antibodies.

Table I. Clinical characteristics of patients with EB virus-positive lymphoepithelial carcinoma arising in the parotid gland since 2005.

First author, year	Age/Sex	Symptom duration, months	Size, mm	FNAC	Stage	Neck node	Treatment	Prognosis (months)	(Refs.)
Saqui-Salces, 2006	56/F	72	25	Biphasic neoplasm	III	+	PD + ND, RT	ANED (108)	(7)
Saqui-Salces, 2006	28/F	36	15	Poorly diff. ca.	IVa	+	CT	DOD (18)	(7)
Manganaris, 2007	67/F	12	55x42x24	Pleomorphic adenoma	III	-	PD, RT	ANED (12)	(8)
Gupta, 2012	40/F	12	25x22x17	Reactive lymphoid cells	II	-	PD		(9)
Spencer, 2012	27/F	12		Lymphoma		-	PD		(10)
Tang, 2012	29/F	10	41x29x37	Poorly diff. ca.	IVa	+	PD + ND, RT		(11)
Kim, 2017	44/M	12	19x17x19	Squamous cell ca.	I	-	PD	ANED (60)	(12)
Kim, 2017	35/F	36	17x15x18		I	-	PD	ANED (60)	(12)
Topal, 2017	66/F	36	93x66x45	Ca.	IVb	-	PD + ND	DOD (48)	(13)
Maeda, 2018	21/M	4	20x20	Negative finding	IVa	+	CRT	ANED (60)	(14)
Halder, 2018	41/F	5		Poorly diff. ca.		+	PD + ND	DOD (3)	(15)
Halder, 2018	47/M					+	PD + ND, RT		(15)
Whaley, 2020	52/F	4	33		IVa	+	PD	DOD (50)	(16)
Whaley, 2020	60/F	3	30		IVa	+	PD, CRT	ANED (112)	(16)
Whaley, 2020	50/F	12	15		I	-	PD, RT	ANED (19)	(16)
Whaley, 2020	53/F	11	16		I	-	PD	DOD (73)	(16)
Whaley, 2020	54/M	3	45		IVb	+	PD, RT	ANED (6)	(16)
Whaley, 2020	59/M	7	42		IVb	+	PD, CRT	AWM (21)	(16)
Lv, 2021	27/M	24			IVb	+	CRT	ANED (6)	(17)
Lv, 2021	33/M	6			IVb	+	CRT	ANED (50)	(17)
Chou, 2022	48/M		16x12		IVa	+	PD + ND, CRT	ANED (163)	(18)
Chou, 2022	51/F		20x12		II	-	PD, RT	ANED (120)	(18)
Chou, 2022	44/M		30x18		II	-	PD, RT	ANED (54)	(18)
Chou, 2022	47/F		20x15		IVa	+	PD + ND, CRT	DOD (40)	(18)
Chou, 2022	31M		24x17		IVa	+	PD + ND, CRT	ANED (8)	(18)
Chou, 2022	27F		25x18	Cytologic atypia	II	-	PD + ND, RT	ANED (4)	(18)
Present case	60/F	36	19x12x10	Poorly diff. ca.	I	-	PD + ND, RT	ANED (20)	-

F, female; M, male; ca., carcinoma; +, present; -, not present; PD, parotidectomy; ND, neck dissection; RT, radiotherapy; CT, chemotherapy; CRT, chemoradiotherapy; ANED, alive with no evidence of disease; DOD, dead of disease; AWM, alive with metastasis; FNAC, fine-needle aspiration cytology; diff, differentiated. Stage was indicated on the 8th edition of the AJCC/TNM staging system.

Somatic mutations have been reported at a low frequency but have been widely distributed among cancer-related genes such as *TP53* in 9.5%, *SYNE1* in 7.9%, *MLL2* in 5.5%, *PIK3CA* in 4.7%, *ARID1A* in 3.9%, *FGFR2* in 3.9%, *NOTCH3* in 3.9% in NPC (6). Little is known about somatic mutation for LEC arising in the parotid gland. Negative results were obtained in the present case, with no mutations identified using a targeted amplicon-based NGS panel of the major cancer-related genes. Somatic mutations in genes other than we analyzed by the DNA-based platform or gene arrangements could possibly be related to the tumorigenesis in LEC.

The mainstay of treatment of parotid LEC is surgical resection with adequate safety margins for patients with resectable tumor (3). Twenty-three of 27 patients (85%) reported were treated with excision as described by a variety of terminologies for the parotid surgery (Table I). Neck dissection was added in 9 of 23 patients (39%). Owing to its high radiosensitivity, postoperative radiotherapy may offer significantly improved survival compared to surgery alone (12,21,22), although no standard of therapy has not yet been proposed. Postoperative radiotherapy was performed in 17 of 23 patients (74%). Three of 27 patients (11%) had unresectable LEC and were treated with chemoradiotherapy. Platinum-based chemotherapy was administered for the patients with advanced-stage disease (14,17). In terms of prognosis, a 5-year survival rate of 75-86% has been reported in patients treated by combined surgery (including neck dissection) followed by radiotherapy (1,21). Six of 23 patients (26%) were died of LEC, mainly due to metastasis to the lungs, bone, and liver. EBV-associated NPC showed abundant lymphocytic infiltration to the tumor and high expression of programmed death-ligand 1 (PD-L1) (23), suggesting the utility of programmed death-1 (PD-1)/PD-L1 inhibitors in patients with advanced stage of NPC. There may be a possible role of immune checkpoint inhibitors in advanced LEC as well.

In conclusion, we report a rare case of LEC arising in the parotid gland. No recurrence was observed as of 20 months after superficial parotidectomy and postoperative radiotherapy. No mutations of major cancer-related genes were identified using NGS. One limitation of this report was that type of latency of EBV could not be analyzed for the LEC. EBV-associated NPC is categorized into type II latency infection in which EBV-encoded nuclear antigen (EBNA)-1 and latent membrane protein (LMP)-1 are expressed, and EBNA-2 is absent (24). Further analysis would be needed to confirm the type of latency by testing the expression of EBV-related antigens for EBV-associated tumors.

Acknowledgements

Not applicable.

Funding

No funding was received.

Availability of data and materials

The datasets generated and/or analyzed during the current study are not publicly available due to privacy reasons but are available from the corresponding author on reasonable request.

Authors' contributions

AK, NB and TG conducted the surgery and provided bedside care. AK, NB and HT drafted the manuscript. KIM performed radiation therapy. TY and HT performed cytologic diagnosis. YK performed mutational analyses. HN performed pathologic investigations. AK and NB confirm the authenticity of all the raw data. All authors read and approved the final manuscript.

Ethics approval and consent to participate

All procedures performed on patient tumor samples in this study were conducted in accordance with the ethical standards of the 1964 Declaration of Helsinki and its later amendments or comparable ethical standards. The present study was approved by the Ethics Committee of Hokuto Hospital (approval no. 1078; Obihiro, Japan).

Patient consent for publication

Written informed consent for publication of clinical details and images was obtained from the patient and her family.

Competing interests

The authors declare that they have no competing interests.

References

1. Seethala R, Thompson LDR, Wenig M, Nagao T and Whaley RD: Lymphoepithelial Carcinoma. In: WHO Classification of Head and Neck Tumours. Skalova A, Hyrcza MD and Mehrotra R (eds). 5th edition. IARC Press, Lyon, 2022.
2. Zhang C, Gu T, Tian Z, Wang L, Han J, Hu Y, Xia R and Li J: Lymphoepithelial carcinoma of the parotid gland: Clinicopathological analysis of 146 cases from a single institute. Head Neck 44: 2055-2062, 2022.
3. Thompson LDR and Whaley RD: Lymphoepithelial carcinoma of salivary glands. Surg Pathol Clin 14: 75-96, 2021.
4. Salivary Gland Cancer Stages: American Joint Committee on Cancer (AJCC) Staging Manual. 8th edition. Springer, New York, NY, pp95, 2017. Available from: https://www.cancer.org/cancer/salivary-gland-cancer/detection-diagnosis-staging/staging.html.
5. Kono M, Bandoh N, Matsuoka R, Goto T, Akahane T, Kato Y, Nakano H, Yamaguchi T, Harabuchi Y and Nishihara H: Glomangiopericytoma of the nasal cavity with CTNNB1 p.S37C mutation: A case report and literature review. Head Neck Pathol 13: 298-303, 2019.
6. Lin DC, Meng X, Hazawa M, Nagata Y, Varela AM, Xu L, Sato Y, Liu LZ, Ding LW, Sharma A, *et al*: The genomic landscape of nasopharyngeal carcinoma. Nat Genet 46: 866-871, 2014.
7. Saqui-Salces M, Martinez-Benitez B and Gamboa-Dominguez A: EBV+ lymphoepithelial carcinoma of the parotid gland in Mexican Mestizo patients with chronic autoimmune diseases. Pathol Oncol Res 12: 41-45, 2006.
8. Manganaris A, Patakiouta F, Xirou P and Manganaris T: Lymphoepithelial carcinoma of the parotid gland: Is an association with Epstein-Barr virus possible in non-endemic areas? Int J Oral Maxillofac Surg 36: 556-559, 2007.
9. Gupta S, Loh KS and Petersson F: Lymphoepithelial carcinoma of the parotid gland arising in an intraglandular lymph node: Report of a rare case mimicking metastasis. Ann Diagn Pathol 16: 416-421, 2012.
10. Spencer CR, Skilbeck CJ, Thway K and Nutting CM: Lymphoepithelial carcinoma of the parotid gland: A rare neck lump. JRSM Short Rep 3: 28, 2012.
11. Tang CG, Schmidtknecht TM, Tang GY, Schloegel LJ and Rasgon B: Lymphoepithelial carcinoma: A case of a rare parotid gland tumor. Perm J 16: 60-62, 2012.
12. Kim YJ, Hong HS, Jeong SH, Lee EH and Jung MJ: Lymphoepithelial carcinoma of the salivary glands. Medicine (Baltimore) 96: e6115, 2017.

13. Topal O and Erinanc H: Coexistence of lymphoepithelial carcinoma of the parotid gland and submandibular gland pleomorphic adenoma. J Craniofac Surg 28: e453-e454, 2017.
14. Maeda H, Yamashiro T, Yamashita Y, Hirakawa H, Agena S, Uehara T, Matayoshi S and Suzuki M: Lymphoepithelial carcinoma in parotid gland related to EBV infection: A case report. Auris Nasus Larynx 45: 170-174, 2018.
15. Halder A, Sommerville J and Gandhi M: Primary lymphoepthelial carcinoma of the parotid gland, pictorial review of a rare entity. J Med Imaging Radiat Oncol 62: 355-360, 2018.
16. Whaley RD, Carlos R, Bishop JA, Rooper L and Thompson LDR: Lymphoepithelial carcinoma of salivary gland EBV-association in endemic versus non-endemic patients: A report of 16 cases. Head Neck Pathol 14: 1001-1012, 2020.
17. Lv S, Xie D, Wu Z, Wang L and Su Y: Is surgery an inevitable treatment for advanced salivary lymphoepithelial carcinoma? Three case reports. Ear Nose Throat J 100: NP402-NP406, 2021.
18. Chou CT, Ou CY, Lee WT and Hsu HJ: Clinical features in salivary gland lymphoepithelial carcinoma in 10 patients: Case series and literature review. Laryngoscope Investig Otolaryngol 7: 779-784, 2022.
19. Hipp JA, Jing X, Zarka MA, Schmitt AC, Siddiqui MT, Wakely P Jr, Bishop J and Ali SZ: Cytomorphologic characteristics and differential diagnoses of lymphoepithelial carcinoma of the parotid. J Am Soc Cytopathol 5: 93-99, 2016.
20. Bauer M, Jasinski-Bergner S, Mandelboim O, Wickenhauser C and Seliger B: Epstein-Barr virus-associated malignancies and immune escape: The role of the tumor microenvironment and tumor cell evasion strategies. Cancers (Basel) 13: 5189, 2021.
21. Zhan KY, Nicolli EA, Khaja SF and Day TA: Lymphoepithelial carcinoma of the major salivary glands: Predictors of survival in a non-endemic region. Oral Oncol 52: 24-29, 2016.
22. Deng DF, Zhou Q, Ye ZM, Xu Z and Shen L: Clinical analysis of 12 patients with primary lymphoepithelial carcinoma of the parotid gland. Eur Arch Otorhinolaryngol 279: 2003-2008, 2022.
23. Hsu MC, Hsiao JR, Chang KC, Wu YH, Su IJ, Jin YT and Chang Y: Increase of programmed death-1-expressing intratumoral CD8 T cells predicts a poor prognosis for nasopharyngeal carcinoma. Mod Pathol 23: 1393-1403, 2010.
24. Fåhraeus R, Fu HL, Ernberg I, Finke J, Rowe M, Klein G, Falk K, Nilsson E, Yadav M, Busson P, *et al*: Expression of Epstein-Barr virus-encoded proteins in nasopharyngeal carcinoma. Int J Cancer 42: 329-338, 1988.